

Computer Aided Diagnosis for Spitzoid lesions classification using Artificial Intelligence techniques

Abir Belaala

LINFI Laboratory , Biskra University.

Labib Sadek Terrissa

LINFI Laboratory , Biskra University.

Noureddine Zerhouni

FEMTO-ST Institute, CNRS - UFC / ENSMM / UTBM, Automatic Control and Micro-Mechatronic Systems

Christine Devalland

Service of Anatomy and Pathology Cytology

ABSTRACT

Spitzoid lesions may be largely categorized into Spitz Nevus, Atypical Spitz Tumors, and Spitz Melanomas. Classifying a lesion precisely as Atypical Spitz Tumors or AST is challenging and often requires the integration of clinical, histological, and immunohistochemical features to differentiate AST from regular Spitz nevus and malignant Spitz melanomas. Specifically, this paper aims to test several artificial intelligence techniques so as to build a computer aided diagnosis system. A proposed three-phase approach is being implemented. In Phase I, collected data are preprocessed with an effective Synthetic Minority Oversampling TEchnique or SMOTE-based method being implemented to treat the imbalance data problem. Then, a feature selection mechanism using genetic algorithm (GA) is applied in Phase II. Finally, in Phase III, a ten-fold cross-validation method is used to compare the performance of seven machine-learning algorithms for classification. Results obtained with SMOTE-Multilayer Perceptron with GA-based 14 features show the highest classification accuracy (0.98), a sensitivity of 0.99, and a specificity of 0.98, outperforming other Spitzoid lesions classification algorithms.

Keywords: Spitz Nevus (SN), Atypical Spitz Tumors (AST), Genetic Algorithm (GA), SMOTE (Synthetic Minority Oversampling Technique), Support Vector Machine (SVM), Logistic Regression (LR), Naïve Bayes (NB), Decision Tree (DT), Random Forest (RF), Multi-Layer Perceptron (MLP), k-Nearest Neighbors (kNN)

Computer Aided Diagnosis for Spitzoid lesions classification using Artificial Intelligence techniques

1. INTRODUCTION

Spitz nevus, a rare form of skin mole, tends to affect mostly young people and children with some 2016 statistics claiming that about 7 out of every 100,000 individuals may be inflicted (Pedrosa, et al., 2016). Typically, patients diagnosed with Spitz nevus are under 21 years old (Sulit, et al., 2007). Historically, such tumors had been treated as a melanoma, identifying with the name, *Benign juvenile melanoma*; later on, Dr. Sophie Spitz, a pathologist, characterized a new class of melanocytic tumor, which has now been popularized as Spitz nevus (Spitz, 1948). According to Harms, et al. (2015), these Spitzoid melanocytic lesions may be clustered into three main types: (a) Spitz nevi; (b) Atypical Spitz Tumors; and (c) Spitzoid Melanomas (SM).

Figure 1 shows two dermoscopic images with **Figure 1A** exhibiting Spitz nevus (SN), and **Figure 1B** depicting Atypical Spitz tumor (AST). Although clinically indistinguishable, these lesions share some dermoscopic as well as histologic features (see **Table 1**). Arguably, the exact clinico-pathologic definition of AST is still particularly challenging for dermatopathologists. Yet, the debate concerning AST prognosis is of highest priority, as their compartment cannot be easily predicted. SN displays a definite benign behavior, whereas SM is malignant and particularly aggressive (Moscarella, et al., 2015). Consequently, Spitzoid lesions, a subset of melanocytic skin lesions, are not only difficult to diagnose from a clinical viewpoint, but from both histological and/or dermoscopic perspectives as well.

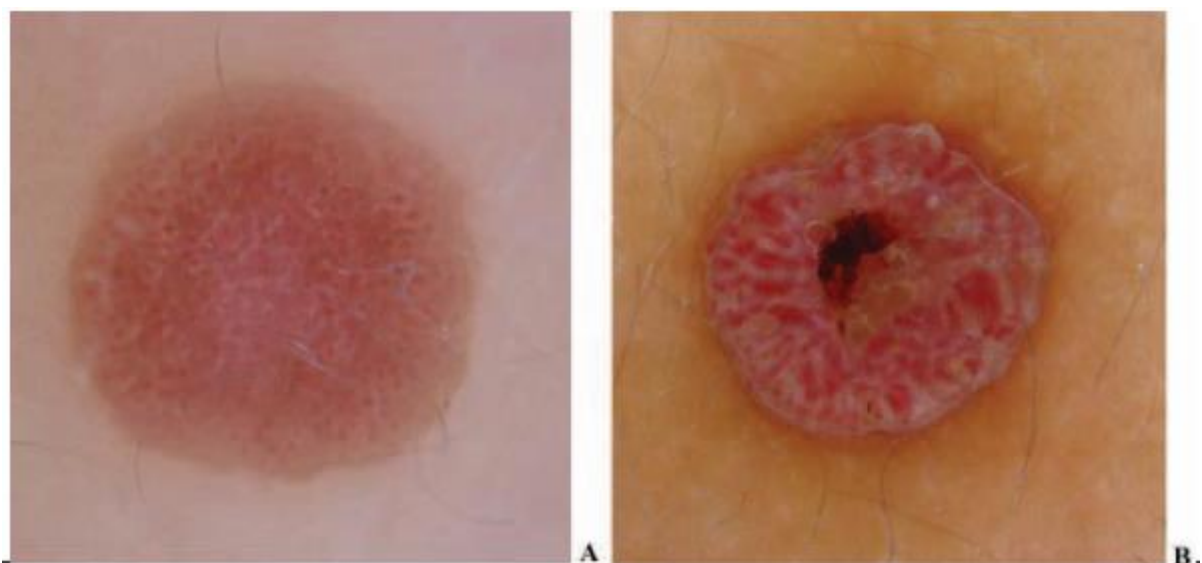


Figure 1: Example dermoscopic images of Spitz Nevus (**1A**), and Atypical Spitz Tumors (**1B**)

Source: Rubegni et al. (2016)

Blum, et al. (2003) argue that SN is diagnosed typically by dermatologists conducting visual inspections of mole using clinical assessment tools such as ABCDE (Asymmetry, Border, Color, Diameter, and Evolution). Even so, a biopsy laboratory examination is often ordered to remove all or part of the mole so as to support the diagnosis. Indeed, a skilled and trained pathologist must be engaged to diagnose a sample, differentiating it between SN v. a more severe melanoma. Consider the similarities of these lesions and the dependency on the skill level of the dermatologist and/or pathologist to inform the diagnostic process, accurate diagnosis remains a problem. Data mining (DM) techniques have been successfully applied to situations where such complexity exists, and the availability of advanced artificial intelligence (AI) techniques and data pre-processing techniques to build computer aided diagnostic (CAD) system can combine to provide effective solutions for the analysis of Spitzoid lesions.

Table 1: Spitz nevus (SN) v. Atypical Spitz tumors (ASTs) v. Spitz melanoma (SM)

Source: Adapted from World Health Organization (2018)

	Spitz nevus	Atypical Spitz tumor	Malignant Spitz tumor
Clinical features	Mean and median age 21 years (range 2-69 years)	Can occur at any age, more common in younger patients (<40 years)	Can occur at any age (often >40 years)
	Most commonly affects extremities	Occur in extremities, trunk	Occur in extremities, trunk, asymmetrical
	Pink or reddish plaque, papule, or nodule	Plaque or nodule Color variegation	Enlarged Plaque or nodule Color variegation Changing lesion
Histopathology	<5 to 6 mm	Often >5 to 10 mm	>5 mm, Often >10 mm
	Symmetrical	Symmetrical or Asymmetrical	Often Asymmetrical
	Well circumscribed	Well or poorly circumscribed	Often poorly circumscribed
	Epidermal hyperplasia	Ulceration possible	Ulceration
	Vertically oriented nests with clefting	Irregular nesting	Irregular and confluent nesting
	Central focal pagetoid spread	Increased cellularity	pagetoid spread may be extensive
	Often wedge-shaped	Greater pagetoid spread than in spitz	Ulceration

		nevus	
	Maturation of dermal component	Deeper dermal than in spitz nevus Maturation may be partial or absent	Effacement of epidermis Lack of maturation
		2-6 dermal mitoses /mm ² Deep mitoses Possible necrosis	Often >6 dermal mitoses /mm ² Deep / marginal or atypical mitoses Necrosis

Notably, the majority of the proposed methodologies in the CAD literature for differentiating among skin lesions has been based chiefly on dermoscopic vision, and often fails to take into account the clinical, genetic, molecular, and immunohistochemical information in making a holistic diagnosis. The primary goals and contributions for this work include: (a) an effort to specify the exact type of a Spitz lesion, which is extremely difficult and challenging, and to the best of our knowledge, no one has used AI to classify them before; (b) an attempt to extend past research results on the steps needed for the development of an automatic diagnostic system for Spitzoid lesion classification; and (c) a move towards integrating clinical, histological, and immunohistochemical features to make accurate diagnosis in distinguishing between SN v. AST, and finding out the impact of these features on the classification.

Broadly, this study evaluates various AI methods to classify Spitz lesions. Specific methods include Decision Tree (DT), Support Vector Machine (SVM), Random Forest (RF), k-Nearest Neighbors (kNN), Naïve Bayes (NB), Logistic Regression (LR), and Multi-Layer Perceptron (MLP), all of which have been commonly used in medical classification problems. Additionally, advanced pre-processing techniques and feature selection methods will be applied to improve the data quality and solve the imbalanced data problem, which will not only lead to a sizable improvement of the prediction time and classification accuracy, but will also cleverly inform on the impact of histological and immunohistochemistry features on the classification.

The rest of this paper is organized as follows. Section II highlights the study background, offering detailed description on the proposed method used in three phases: (a) the preprocessing phase; (b) the feature selection phase; and (c) the classification phase. Section III highlights the key indicators, including performance measure(s), accuracy, sensitivity, specificity, G-mean, F-measure, ROC curve, and area under the ROC curve (AUC) as well as overviews the experimental findings. In Section IV, a discussion of the comparative analysis is presented. Finally, Section V concludes the study with a brief look at various limitations and potential future works.

2. BACKGROUND

In recent years, computer scientists have diverted attention to skin lesion analysis. A great majority of the proposed methodologies in the extant literature aims to develop a CAD to assist dermatopathologists to make accurate diagnosis, thereby achieving a proper decision. Specifically, Al-Masni et al. (2018) suggest a segmentation method on dermoscopic images using full resolution convolutional networks (FrCN). Also, they argue that the proposed technique is able to generate full spatial resolution features for each pixel of the input dermoscopy images. In contrast, a 3D skin lesion reconstruction technique using the estimated depth obtained from regular dermoscopic images, and the adaptive snake technique in the segmentation phase have been proposed by Satheesha, et al. (2017). Here, by fitting the depth map estimated to the underlying 2D surface, a 3D reconstruction can be achieved. This is then followed by a feature extraction (Color, texture and 2D shape) and feature selection to study the effects of features on decision-making. Finally, AdaBoost and SVM classifiers can be applied in the classification phase.

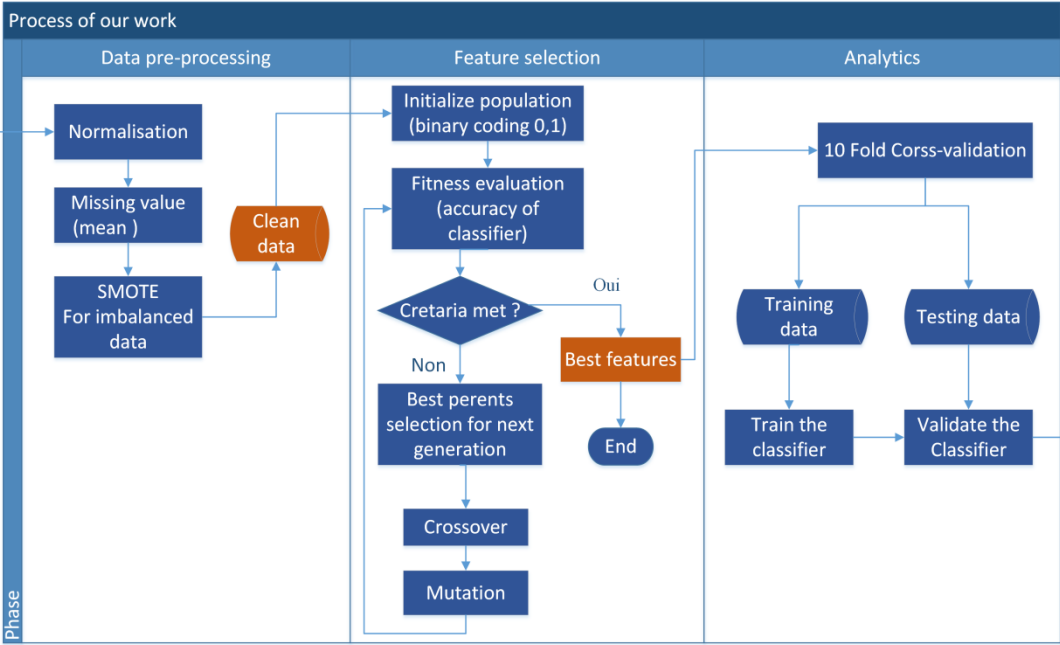
In Jain, et al. (2015), a CAD for the diagnosis of Melanoma Skin Cancer on dermoscopic Image Processing is presented. In Roffman, et al. (2018), a multi-parameterized artificial neural network (ANN) using available personal health dermoscopic images for early detection of non-melanoma skin cancer with high sensitivity and specificity has been developed.

Finally, in Xie, et al. (2017), a novel method for the classification of melanocytic tumors as benign v. malignant using digital dermoscopy images has been advanced; specifically, in the feature extraction and reduction phase, the Principal Component Analysis (PCA) technique is used whereas in the classification phase, a NN meta-ensemble model is applied by combining fuzzy NNs with Back Propagation NNs and evaluating the performance of the proposed method using fuzzy NNs, RFs, Gentle Adaboost, k-NN, two SVM methods, and two systems using the Bag-of-Features (BoF) classification model.

2.1 Proposed method

Figure 2 shows the general schematic diagram of the proposed study technique. The details of each processing stage are now described in the subsequent sections.

Figure 2: General schema of our proposed process



2.1.1 Data description

A retrospective study of 54 Spitz lesions diagnosis from 2000 to 2018 has been conducted in the pathology department of Nord Franche Comte hospital (France). The cohort comprises 47 SN and 7 AST performed by five pathologists. As described in **Table 2**, the dataset contains 29 attributes. These attributes are computed from clinical, histological and immunohistochemical data, details of which are shown in **Table 3**.

Table 2: Description of Spitz nevus Dataset

Dataset	No. Of Attributes	No. Of Instances	No. Of Classes
Spitz database	29	54	2 (47 SN & 7 AST)

Table 3: Spitz nevus dataset details

		Feature	Input type	Input range	Details
Clinical data	1	Gender	Binary	0 or 1	Man : 0 Women: 1
	2	Localization	quinary	1 or 2 or 3 or 4 or 5	1:Trunk, 2:Lower extremity, 3:Upper extremities, 4:abdo 5:Face and neck
	3	Age	Continuous	From 2 to 54	Majority of them are under 20 years old
Histology data	4	Format	Ternary	1or 2 or 3	1: junctional, 2: wholly dermal. 3: compound
	5	Size of spitz	Continuous	From 0.3 to 1.4	only 5 patients more than 1 cm , the rest under 1 cm
	6	Thickness	Continuous	From 0.1 to 6	Majority < 2,5 mm
	7	Mitotic index		From 0 to 2.2	Majority < 0,5 per mm square
	8	Cytonuclear Atypia	Binary	0 or 1	0: no 1: yes
	9	deep mitosis			
	10	Atypical Mitosis			
	11	Infiltration of the hypodermis			
	12	Asymmetry			
	13	Blurred boundaries			
	14	Pagetoid spread			
	15	Density of lymphocytic infiltrate			
	16	Hypercellularity			
	17	Ulceration			
	18	Kamino's body			
19	desmoplastic cells				
20	epidermal alteration				
21	grenz zone infiltration				
22	irregular nests				
23	lack of maturation				
Immunohistochemistr	24	P16			100% no loss
	25	KI 67	Continuous	From 0 to 18	most of them < 5
	26	BRAF	Binary	0 or 1	0: mute, 1: not mute

27	ALK IH	Binary	0 or 1	0: negatif, 1: positif	
28	ALK Fish	Nul	Nul	Nul	
29	Melanin pigmentation	quaternary	0 or 1 or 2 or 3		

2.2 The Pre-Processing Phase

In order to achieve more accurate results, data pre-processing entails a critical step in transforming raw SN data into a clean and understandable format for analysis. The following sub-sections discuss techniques applied to improve the quality of our dataset.

2.2.1 Categorical data

First, the majority of features in our dataset is categorical (**Table 3**). As machine-learning models are based on mathematical equations, we would only use numbers in the equations, which will then be converted into numerical values.

2.2.2 Missing values

In health analytics, missing data may be unavoidable due to a variety of reasons, for example, faulty equipment, and/or imprecise or lost measurements; moreover, the errors of the caregivers, for instance, physicians or nurses who forget and/or improperly record the information may also lead to missing information. Yet, the most serious problems of missing values are the resulting consequences, thereby effectively slowing down the analytic processing due to lower efficiencies, and/or the potential to compromise the information extracted from the data, thereby leading to faulty conclusions.

Essentially, three strategies may be applied to deal with missing data. The first is missing data ignoring techniques that simply delete the cases that comprise the missing data (Houari, et al., 2016). In cases where the size of the data is small (as with the current study), deleting any information is not ideal. The second approach would be to deploy missing data modeling techniques. The strategy here is to define a model from the existing data and then generate inferences based on the distribution of the data (Houari, et al., 2016). The third strategy is to employ the missing data imputation techniques. These techniques complete the missing data in the dataset with a potential value (Cleophas, et al., 2016). Examples of such techniques include: Mean regression, K-NNs, and multiple imputations. In the current work, we apply the Mean imputation, one of the most commonly used methods, by replacing the missing value with the total sample mean. Accordingly, this strategy is simple and easy to implement.

2.2.3 Imbalance data

The imbalance of medical data, as characterized by the non-uniformity of the class distribution among the classes, seriously affects the accuracy of medical diagnosis classification. Data imbalance exists widely in real world datasets, especially those in the medical field. The study dataset is found to be highly unbalanced, comprising 47 cases of classical SN v. only 7 cases of ASTs.

To resolve this challenge, a widely implemented technique for dealing with highly unbalanced datasets is *resampling*. *Resampling* consists of eliminating samples from the majority class (*under-sampling*) and/or adding more examples from the minority class (*over-sampling*). The simplest implementation of over-sampling is to duplicate random samples from the minority class, which can affect over-fitting. In under-sampling (Bach, et al., 2017), the simplest technique is to randomly remove samples from the majority class, which can cause wastage of information. SMOTE (Synthetic Minority Oversampling TEchnique) consists of synthesizing elements for the minority class, based on those that have already existed (Chawla, et al., 2002). It works by randomly picking “k,” a point from the minority class, and computing the k-NNs for this point. Synthetic points are then added between the chosen point and its neighbors.

Other techniques discussed in the extant literature include SVM SMOTE (Nguyen, et al., 2009), or borderline-SMOTE (Han, et al., 2005), where only the minority examples near the borderline are over-sampled. Adaptive synthetic sampling (AdaSyn), as presented in Han, et al. (2008), includes both minority and majority classes in processing and adds extra synthetic samples to the minority class. A comparative study between these resampling techniques is provided in **Table 4**.

<Place **TABLE 4** about here>

2.2.4 Scaling data

In this work, the data columns are rescaled to a range of [0-1] for two reasons:

- (a) to simplify the numerical computational complexities; and
- (b) to get rid of attributes in the bigger numeric range while controlling attributes in the lesser numeric range (Aličković, et al., 2017).

2.3 The Feature Selection Phase

Feature selection is a key step in the SN diagnosis process. As the study dataset typically consists of several features, a critical goal is to identify the most relevant features to the problem at hand. Other advantages of feature selection include cost reduction, increasing classification accuracy, decreasing the complexity of the model, and reducing the learning time (Turgut, et al., 2018).

With far too many attributes specific to the current study dataset, this feature selection process is clearly non-trivial. Indeed, identifying those attributes that are the most relevant to the classification is complicated. To this end, our strategy is to apply a mix of three feature selection methods: filter, wrapper and embedded methods. The filter methods measure the significance of identifiable features by their association with the dependent variable whereas the embedded methods combine the qualities of filter and wrapper methods as implemented by algorithms that have their own built-in feature selection methods. Finally, the wrapper methods measure the effectiveness of a subset of features by actually training a model on the two differing wrapper types: deterministic v. randomize. Herein, we apply the randomize wrapper method via genetic algorithm, which is discussed next.

Genetic Algorithm (GA)

To date, GAs have gained increasing popularity. Characterized by a heuristic and general adaptive optimization search methodology, these algorithms are inspired by the Darwin’s theory of evolution. Initially presented by Bledsoe (Bledsoe, et al., 1961), and mathematically formalized by Holland (Holland, et al., 1992), these GAs operate with diverse populations, with the dominant solution frequently achieved only after a sequence of iterative steps.

These GAs also develop sequential populations of periodic solutions that are presented by a chromosome until adequate results have been reached (Aličković, et al., 2017). These chromosomes are evaluated by a predefined fitness function. Two major operators, which impact on the fitness value, are the crossover and mutation functions. For the next generation, chromosomes that obtained the higher fitness value will have the corresponding higher probability to be selected, using either the roulette wheel or the tournament strategy (Puyalnithi et al., 2018). Genes may be changed randomly in mutation.

The parameter settings for the GA applied herein as feature selection are presented in **Table 4**

Table 4: parameter settings of our genetic algorithm based feature selection

Parameter	Value
Population size	100
Number of generation	50
Rate of crossover	0.8
Rate of mutation	0.1
Fitness evaluation	Accuracy of classifier
Size of chromosome	27
Coding	Binary 0: not selected 1: selected

In the initial population stage, different individual entities are assigned randomly, with binary coding where 1 present the selected feature and 0 not selected. All individual entities have a unique size (27 genes in each chromosome). The chromosomes characterizing the population represent a set of probable optimal features. At each generation, the fitness value of each potential solution is derived from using a tenfold cross-validation method to calculate the accuracy of classifier and then intelligently applied to select the population for the next generation by roulette wheel selection method. In order to stop the solution set falling into a local optimal, crossover and mutation are used to generate populations that represented new sets of solutions.

The basic process of the applied GA may be summarized as follows:

1. *Initial population:* The initial population size is 100 - several different numbers of generations in the experiment are tried and tested, before deciding to use 50 generations, which yields the highest accuracy as depicted in **Figure 3**.
2. *Evaluation:* The fitness value of each population determines if the population will survive in future generations. Herein, the accuracy of the classifier serves as the fitness function.
3. *Selection:* The population with the better fitness value has a greater probability to be selected to the next generation; herein, a roulette wheel mechanism is deployed to choose the population sets for the next generation.
4. *Crossover:* Crossover is the process of generating a new individual entity from two parents by exchanging and reordering their parts. By crossing, the search power of the GA is dramatically increased. To implement the crossover in the study GA-based feature selection, a single-point crossover operator is chosen with a rate of 0.8.
5. *Mutation:* Mutation is the process of changing some gene values of individual sequences to increase the population variety; herein, the mutation with a rate of 0.1 is applied.

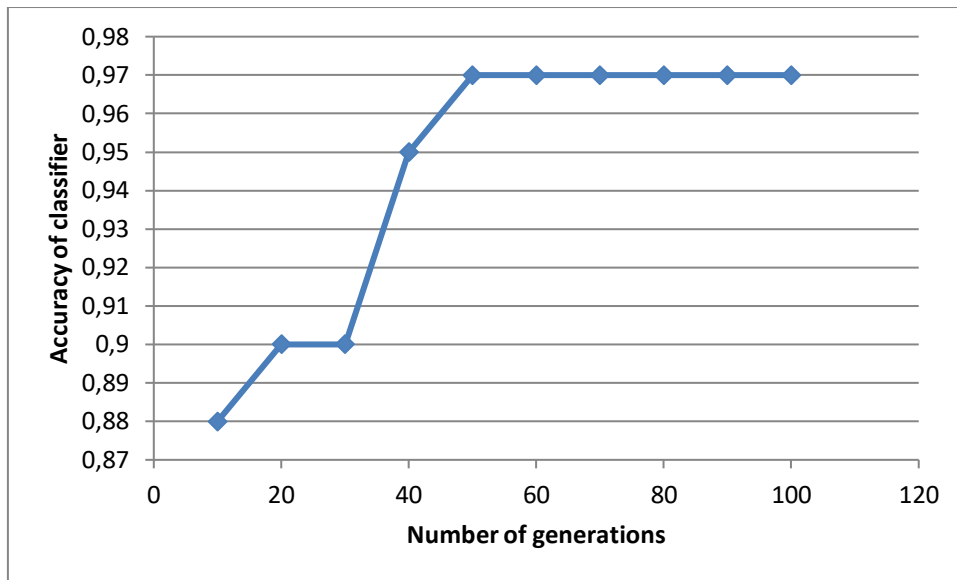


Figure 3: impact of number of generations on accuracy of classifier

2.4 The Classification Phase

The various methods applied for evaluation in the study classification phase are briefly highlighted at this point. These include:

2.4.1 Support Vector Machine (SVM)

SVM, which is based on statistical learning theory and the structural risk minimization principle, has been used for classification and regression (Vapnik et al., 1998). The main SVM concept that is applied here is to map the input data from the N-dimensional input space, through some non-linear mapping. Then, to classify our data we should determine the optimal hyperplane that maximizes the margins of class boundaries.

2.4.2 Decision Tree (DT)

DT, a popular and the most powerful supervised learning methods for classification where each internal node signifies a check on an attribute, is applied herein. Each branch of the DT represents a result of the check, and each leaf node contains a class label. A DT algorithm is implemented by generating a DT with terminal nodes as the class label (Classical Spitz Nevus, Atypical Spitz Tumors). Additionally, sets of if-then conditions are employed to classify novel samples.

2.4.3 Logistic Regression (LR)

The LR model originates as a result of modeling the posterior probability of K classes via linear functions in x , while ensuring that the probabilities sum to one and remain in the range $[0, 1]$. The selection of denominator is random in that the estimates are equally distributed under this choice (Aličković et al., 2017). When $K = 2$, as would be in our case (SN, AST), the model is straightforward as there is just a single linear function.

2.4.4 Naïve Bayes (NB)

Bayesian Network describing sets of local conditional probabilities together with a set of conditional independent assumptions is applied herein to clarify the joint probability distribution for a set of variables. In the NB network, each node shows variable in the joint space; for all variables, two types of information are detailed. First, the variable is definitely independent of its non-descendants in the network given its instant predecessors in the network. Second, a conditional probability table is given for each variable, indicating the probability distribution of this variable assuming the values of its instantaneous antecedents (Gambhir et al., 2018).

2.4.5 K-Nearest Neighbor (kNN)

The basic concept of kNN is to compute the minimum distance between the stored feature vectors and the new feature vectors. Firstly, we compute the distances between all samples that have already been classified into clusters; then, we find the k samples with the smallest distance values; and finally, we approve the new data. Note that a new sample will be classified to the largest cluster among the selected k samples (Ebrahimzadeh et al., 2019). We tried the values of k from 1 to 10 and found that $k = 3$ offers the best results with this classifier as highlighted in **Figure 4**.

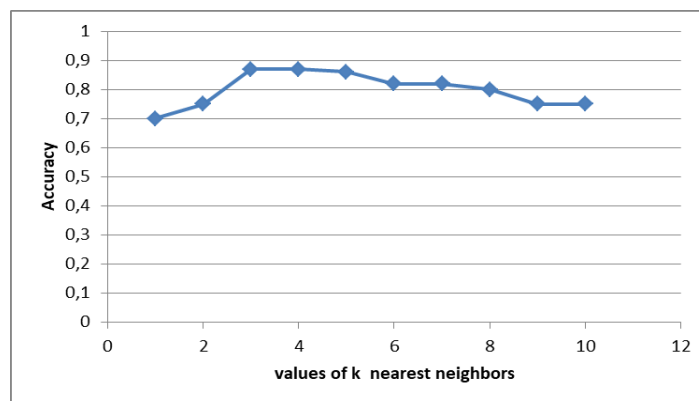


Figure 4: the change of Accuracy in terms of nearest neighbor's k value

2.4.6 Multilayer Perceptron (MLP)

The MLP classifier applied herein has a three-layer structure as shown in **Figure 5**. The size of the input layer is equal to the number of the selected features ($1 < N < 27$). In contrast, the output layer contains one node for a possibility of only 2 classes to be classified (SN v. AST). Additionally, having selected and trained all potential combinations of the selected number of neurons in the hidden layer, we found the optimized number to be 50. We also added an activation function to make our MLP flexible vis-à-vis the learning of the non-linear decision boundaries. There are several kinds of activation function discussed in the extant literature; herein, we used the Rectified Linear Units (ReLu), which is one of the popular activation functions.

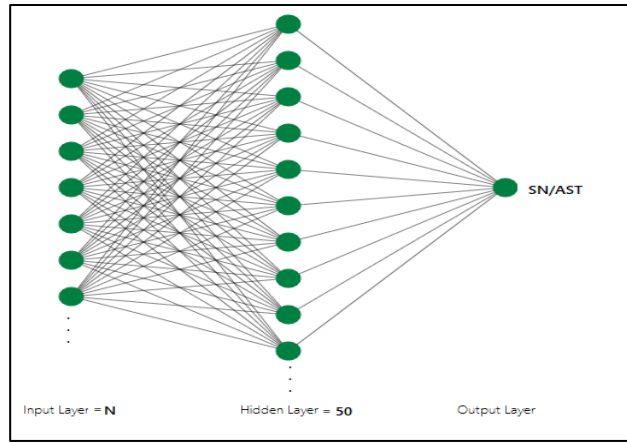


Figure 5: Our multi layer perceptron (MLP) architecture

2.4.7 *Random Forest (RF)*

RF has been defined by (2001, Breiman, et al) as the “combination of tree predictors such that each tree depends on the values of a random vector sampled independently and with the same distribution for all trees in the forest.” Herein, when RF is used to perform the classification task, a class vote from each tree is generated and the majority vote is then used to perform the classification task.

3. PERFORMANCE METRICS & EXPERIMENTATION

In this section, the various performance metrics applicable for evaluating and interpreting multiple experimental results are first highlighted prior to discussing the study findings and their interpretations. Notably, we conduct the experiments in the python language environment, and when no parameter values are given, the default values of these functions will apply.

3.1 Performance Metrics

A tenfold cross-validation scheme is performed to evaluate and compare the performance of all of the aforementioned classification methods being applied. One of the major issues when dealing with unbalanced datasets relates to the metrics used to evaluate the model’s performance, for example, using simpler metrics like accuracy score alone can be relatively misleading.

Accordingly, a range of different performance metrics is adopted for studying and comparing the various classification models differentiating SN v. AST samples. These metrics entail accuracy, sensitivity, specificity, precision, F-measure, G-mean, ROC and AUC with measures based on the correct and wrong prediction of the classifier.

For the respective metrics, the below formulae are computed with:

TP = True positive means number of SN which are predicted as SN; TN = True negative means number of AST which are predicted as AST; FP = False positive means number of SN which are predicted as AST; and FN= False Negative means number of AST which are predicted as SN.

3.1.1 Accuracy

Accuracy refers to the whole number of instances that may be classified correctly (Yu et al., 2015).

$$Accuracy = \frac{TP+TN}{TN+TP+FP+FN}$$

3.1.2 Sensitivity

Sensitivity measures the quantity of SN instances, which are correctly identified by the classifier.

$$Sensitivity = \frac{TP}{TP+FN}$$

3.1.3 Specificity

Specificity measures the quantity of AST instances, which are correctly identified by the classifier.

$$Specificity = \frac{TN}{TN+FP}$$

3.1.4 Precision

Precision measures the amount of predicted SN that is truly related to the SN class.

$$Precision = \frac{TP}{TP+FP}$$

3.1.5 F-measure

F-measure is a combination of precision and sensitivity. Therefore, a high value of F-measure shows a high value of both precision and sensitivity (Majid et al., 2014).

$$F1\text{-measure} = 2 * \frac{Precision * Sensitivity}{Precision + Sensitivity}$$

3.1.6 G-mean

G-mean is a widely used measure for evaluating the performance of models based on unbalanced data. The evaluation made by the geometric mean of all class recall rates.

$$G\text{-mean} = \sqrt{(Specificity * Sensitivity)}$$

3.1.6 Receiver Operating Characteristics (ROC)

The ROC curve is a graphical plot used to compare the performance of a binary classifier, which in our case would be SN v. AST.

3.1.7 Area Under Curve (AUC)

AUC is calculated for assessing performance of the classifier and provides an examination of the classifier stability and consistency.

3.2 Data Sampling Results

As noted, four different over-sampling methods have been applied with the unbalanced dataset so that their performance may be appropriately compared.

Table 5 (previously shown) details the performance of the different machine learning (ML) classifiers on our dataset with and without oversampling methods.

All classifier's accuracy is high in the case of classifiers without oversampling methods, that is, between 0.72 - 0.87. Thus, each classifier's performance on other performance measures has to be investigated beyond just accuracy. Among the other measures, the sensitivity, specificity, and F-measure show a significant difference between SN (majority - very high) v. AST (minority - very low) classes. Especially with LR, KNN, MLP, and SVM the sensitivity and specificity of AST class is 0.00, which means these classifiers over-fits and the model predicts all cases as SN.

As shown in **Figure 6**, DT and RF gets higher AUC scores than the other classifiers. In order to verify the efficiency of the SMOTE method in handling the problem of unbalanced dataset in the study, we have applied other existing methods as summarized in **Table 5** to compare their performance. The input that needed to be determined in SMOTE method is the number of nearest neighbors "k". We tried several different k values in the experiment, finally deciding on using k = 6, which yields the best accuracy (see **Figure 7**).

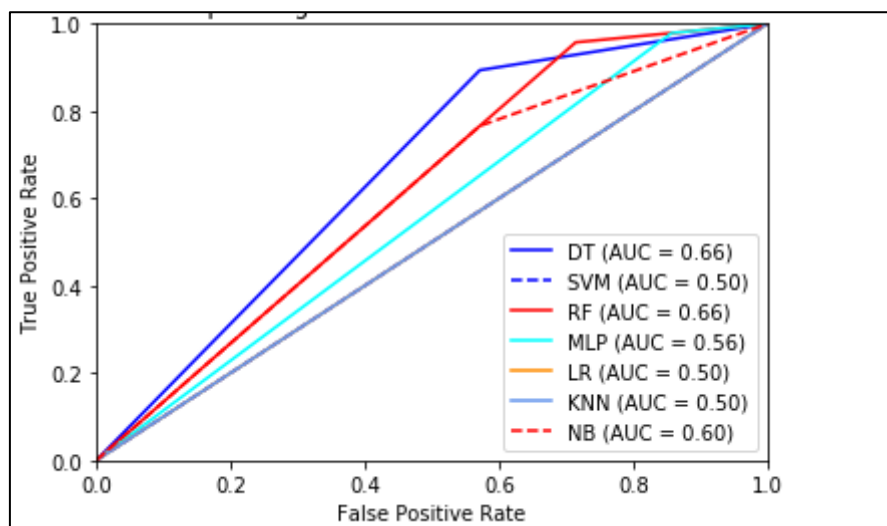


Figure 6: ROC curve of classifiers

Table 5: Experimental performance on our dataset without /with existing over-sampling methods

		Accuracy	Sensitivity		Specificity		F1-measure		G-mean
			AST	SN	AST	SN	AST	SN	
Without Over-sampling methods	DT	0.83	0.43	0.87	0.33	0.91	0.38	0.89	0.65
	RF	0.85	0.14	0.96	0.33	0.88	0.20	0.92	0.85
	SVM	0.87	0.00	1.00	0.00	0.87	0.00	0.93	0.50
	NB	0.72	0.43	0.77	0.21	0.90	0.29	0.83	0.59
	LR	0.87	0.00	1.00	0.00	0.87	0.00	0.93	0.50
	KNN	0.87	0.00	1.00	0.00	0.87	0.00	0.87	0.50
	MLP	0.85	0.00	0.98	0.00	0.87	0.00	0.92	0.48
SMOTE k=6	DT	0.94	0.94	0.85	0.82	0.95	0.88	0.90	0.89
	RF	0.95	0.94	0.94	0.98	0.98	0.96	0.96	0.95
	SVM	0.87	0.85	0.89	0.89	0.86	0.87	0.88	0.87
	NB	0.88	1.00	0.77	0.81	1.00	0.90	0.87	0.88
	LR	0.94	1.00	0.89	0.90	1.00	0.95	0.94	0.94
	KNN	0.70	1.00	0.81	0.65	0.53	0.75	0.64	0.70
	MLP	0.93	1.00	0.87	0.89	1.00	0.94	0.93	0.93
Borderline SMOTE	DT	0.91	0.91	0.94	0.93	0.92	0.92	0.93	0.92
	RF	0.94	0.91	0.98	0.98	0.92	0.95	0.95	0.94
	SVM	0.86	0.85	0.85	0.87	0.87	0.86	0.86	0.86
	NB	0.88	1.00	0.77	0.81	1.00	0.90	0.87	0.88
	LR	0.93	0.94	0.94	0.94	0.94	0.94	0.94	0.93
	KNN	0.73	0.77	0.70	0.72	0.75	0.74	0.73	0.73
	MLP	0.88	0.98	0.79	0.82	0.97	0.89	0.87	0.88
ADASYN	DT	0.94	0.94	0.96	0.96	0.94	0.95	0.95	0.94
	RF	0.94	0.94	0.96	0.94	0.94	0.95	0.95	0.94
	SVM	0.81	0.89	0.74	0.78	0.88	0.83	0.80	0.81
	NB	0.88	1.00	0.77	0.81	1.00	0.90	0.87	0.88
	LR	0.94	1.00	0.89	0.90	1.00	0.95	0.94	0.94
	KNN	0.81	0.61	0.49	0.61	0.72	0.70	0.58	0.64
	MLP	0.93	1.00	0.87	0.89	1.00	0.94	0.93	0.93
SVMSMOTE	DT	0.94	0.93	0.96	0.93	0.96	0.93	0.96	0.94
	RF	0.92	0.87	0.96	0.93	0.92	0.90	0.94	0.92
	SVM	0.76	0.59	0.89	0.80	0.75	0.68	0.82	0.74
	NB	0.82	1.00	0.74	0.64	1.00	0.78	0.85	0.87
	LR	0.92	0.86	0.96	0.90	0.94	0.95	0.88	0.91
	KNN	0.75	0.62	0.83	0.67	0.80	0.64	0.81	0.72
	MLP	0.91	0.97	0.87	0.84	0.98	0.90	0.92	0.92

We now summarize performance of the four oversampling methods: SMOTE, Borderline SMOTE, ADASYN, SVMSMOTE. The results are relatively similar, where we see a balance in sensitivity, specificity, and F-measure of both SN and ASN class. Even so, SMOTE gives the highest accuracy 0.95 and G-mean 0.95 among all oversampling methods with random forest classifier. **Figure 8** depicts the distribution of our data after applying SMOTE.

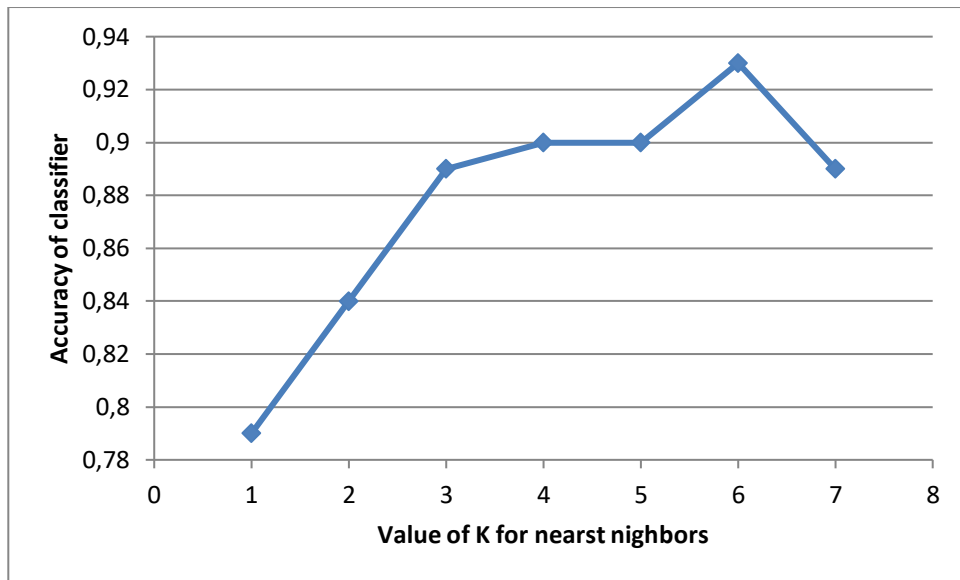


Figure 7: impact of several different SMOTE's k values on the accuracy

The results suggest that the SMOTE method is the best technique to balance our Spitz nevus dataset. **Figure 9** shows the ROC curve of classifiers with the SMOTE technique. Here, we notice a great improvement is achieved with all classifiers. Finally, FR and DT perform better than other classifiers with AUC = 96.

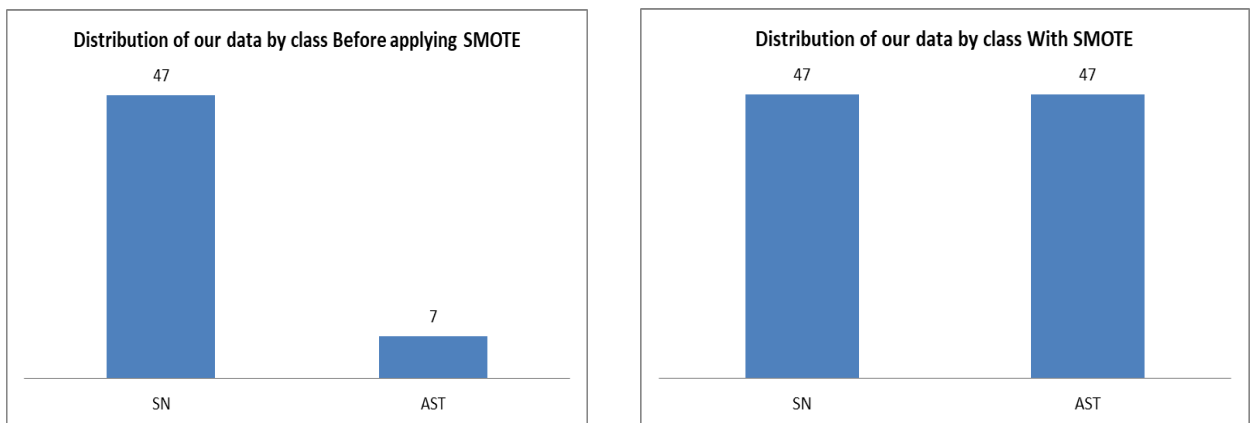


Figure 8: Distribution of our data with/ without SMOTE technique

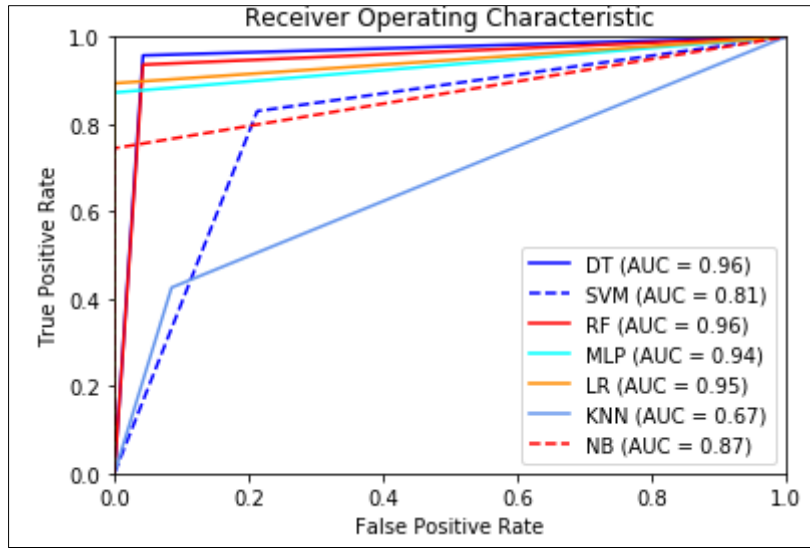


Figure 9: ROC curve of classifiers with SMOTE technique

3.3 Feature Selection Results

In the second test, we first used GA-based feature selection to select the best attributes; then, we used the same ML classifiers as in the previous section.

Table 6 shows the performance of the different ML classifiers on our dataset with and without GA-based feature selection. Experimental results show that the highest classification performances are achieved when GA is used as feature selection with all classifiers. Notwithstanding, the MLP classifier does a good job in predicting the AST instances correctly.

Table 6: Experimental performance on our data without / with genetic algorithm based feature selection

		Accuracy	Sensitivity		Specificity		F1-measure		G-mean
			AST	SN	AST	SN	AST	SN	
Smote Without GA	DT	0.94	0.94	0.85	0.82	0.95	0.88	0.90	0.89
	RF	0.95	0.94	0.94	0.98	0.98	0.96	0.96	0.95
	SVM	0.87	0.85	0.89	0.89	0.86	0.87	0.88	0.87
	NB	0.88	1.00	0.77	0.81	1.00	0.90	0.87	0.88
	LR	0.94	0.87	0.89	0.90	1.00	0.95	0.94	0.94
	KNN	0.70	1.00	0.81	0.65	0.53	0.75	0.64	0.70
	MLP	0.93	1.00	0.87	0.89	1.00	0.94	0.93	0.93
Smote with GA	DT	0.95	0.98	0.94	0.94	0.98	0.96	0.96	0.95
	RF	0.97	1.00	0.96	0.96	1.00	0.98	0.98	0.97
	SVM	0.94	0.98	0.91	0.92	0.98	0.95	0.95	0.94
	NB	0.90	1.00	0.81	0.84	1.00	0.91	0.89	0.90
	LR	0.93	1.00	0.87	0.89	1.00	0.94	0.93	0.93
	KNN	0.94	1.00	0.89	0.90	1.00	0.95	0.94	0.94
	MLP	0.98	1.00	0.98	0.98	1.00	0.99	0.99	0.98

Table 7: feature selection results obtained by different classifiers as fitness evaluation

	GA-DT	GA-SVM	GA-LR	GA-NB	GA-KNN	GA-MLP	GA-RF	
Gender	no	yes	yes	yes	no	no	yes	
Localization	yes	yes	no	yes	no	yes	yes	
Age	no	no	no	yes	no	no	yes	
Format	no	yes	yes	yes	no	no	no	
Diameter	yes	no	yes	yes	no	no	yes	
diameter >1	no	no	yes	yes	no	no	no	
Thickness	no	yes	no	no	yes	no	no	
Mitotic index	no	no	no	yes	no	no	yes	
Cytonuclear Atypia	yes	yes	yes	yes	yes	yes	yes	
mitoses profaned	no	yes	yes	yes	yes	yes	no	
Infiltration of the hypodermis	no	yes	no	no	yes	yes	yes	
Asymmetry	no	yes	yes	no	yes	yes	yes	
Blurred boundaries	yes	no	yes	no	yes	no	no	
Pagetoide migration	no	no	yes	no	no	yes	yes	
hyperCELL	yes	no	yes	yes	no	no	yes	
Kamino's body	no	yes	yes	yes	no	no	no	
Desmo	no	no	yes	no	no	yes	no	
Modif epid	no	yes	yes	yes	no	yes	yes	
Grenz	no	no	no	yes	yes	yes	no	
Th irreg	no	no	yes	yes	no	yes	no	
No grad	no	yes	no	no	yes	yes	yes	
KI 67	yes	no	no	yes	no	no	yes	
Ki67>1%	yes	yes	yes	yes	no	yes	yes	
BRAF	no	yes	yes	no	no	yes	no	
ALK IH	no	yes	yes	no	no	no	yes	
Ly	yes	no	no	yes	no	yes	no	
Pig m�el	no	yes	no	no	no	no	yes	

As shown in **Table 7**, highest accuracy of 0.98, F-measure of 0.99, and G-mean of 0.98 with 14 selected features are attained with the MPL. Here, AUC = 98 as shown in **Figure 10**. Next is RF method with 16 selected features, an accuracy of 0.97, F-measure of 0.98, AUC of 0.98, and G-mean of 0.97. Then, DT comes with accuracy of 0.95, F-measure of 0.94, AUC = 0.95, and G-mean of 0.95. Lastly, LR and NB provide the lowest accuracy of 0.93 and 0.90, respectively.

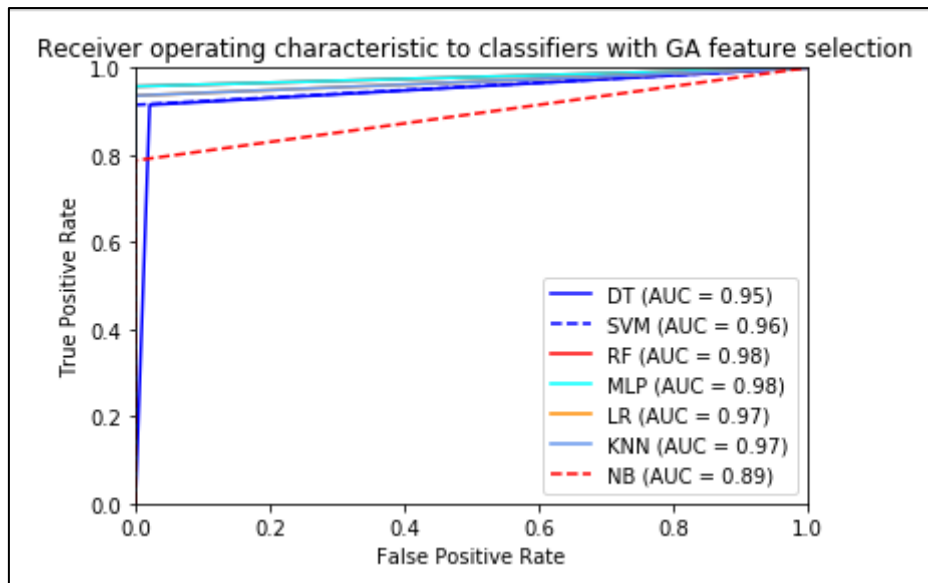


Figure 10: ROC curve of classifiers with GA based feature selection

In **Figure 11**, the bar chart highlights the most selected features with existing classifiers combined with GA as a feature selection method. Overall, for clinical features (colored in red), it is noted that localization is the most important as evidenced by its selection via five classifiers. Gender comes next, whereas only two classifiers have selected “age.” For histology features (colored in blue), it is clear that Cytonuclear Atypia is a most significant feature as selected by all classifiers. Finally, among immunohistochemistry features (colored in green), ki67 marker is the most significant.

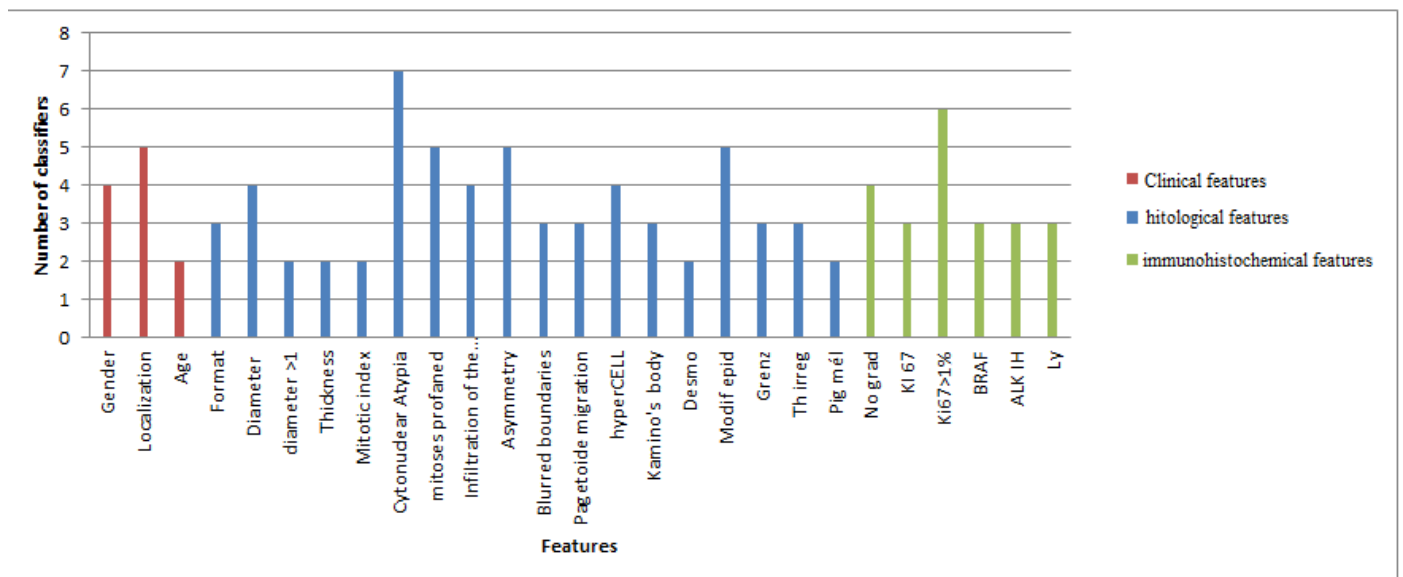


Figure 11: most selected features with existing classifiers as fitness evaluation

Figure 12 shows the performance of the different ML classifiers on our dataset with the number of selected features by GA. Experimental results show that when we used Naïve Bayes (NB) as the classifier with GA, it gave us the highest number of selected feature (17), and lowest accuracy (0.90), which means NB is the worst classifier applied. In contrast, DT offers the lowest number of selected features (8) with

higher accuracy (0.95). Notwithstanding, MLP provides the best classification accuracy (0.98) with 14 features; for this reason, we have chosen MLP as a fitness evaluation and the classifier of choice in our model.

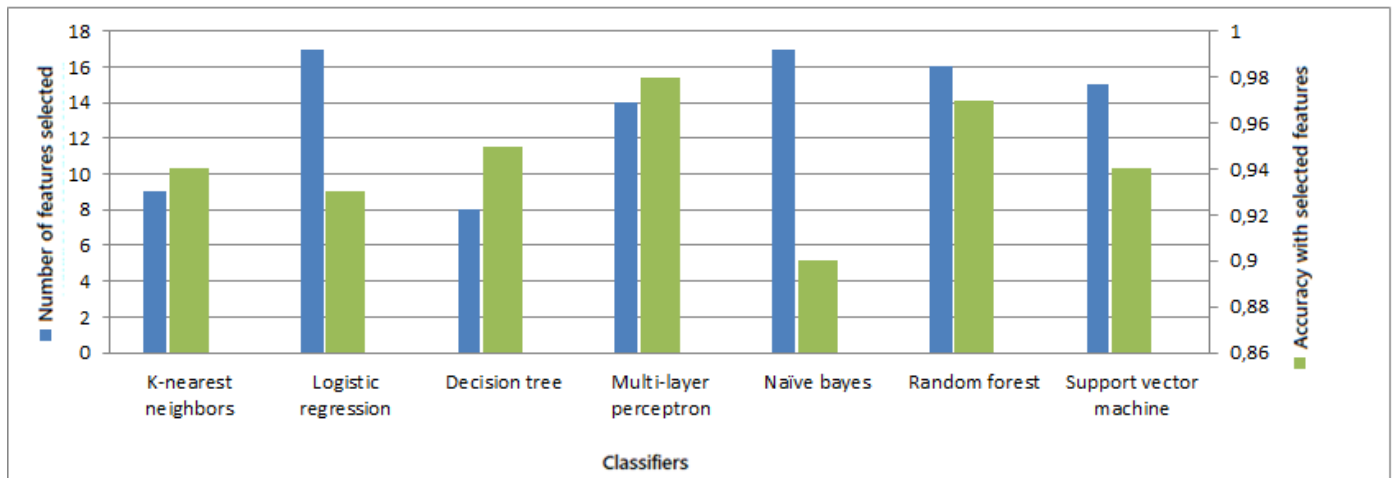


Figure 12: number of selected features by GA and accuracy of classifiers

4. DISCUSSION & CONCLUSION

The motivation for this research is to explore ways to improve the classification performance of different ML algorithms so as to accurately identify Spitz nevus lesions. The research presented here goes about the exploration by first removing class-imbalance in a real-world dataset and refitting then for analysis via the various methods of best features selection.

Different class-imbalance techniques consisting of SMOTE, Borderline SMOTE, ADASYN, and SVMSMOTE were applied. All four class-imbalance techniques have been found to improve the classification results. This is consistent with previous research findings as provided in the cumulated literature (Firoze et al., 2015; Han et al., 2019; Mathew et al., 2018). However, in our case, the SMOTE method outperformed the other techniques. It uses k-nearest neighbors and generates very good prediction results. Furthermore, the features, which are most appropriate for Spitzoid lesions classification, must be utilized as the inputs of the model. For this reason, it is found that GA is an appropriate means for classifying the Spitzoid lesions data to achieve accurate diagnosis.

4.1 Contributions of the Research

This study attempts to analyze Spitzoid lesions related to clinical, histological, and immunohistochemical features using AI techniques. Seven (7) types of classifiers: K-NN, LR, DT, MLP, NB, RF, and SVM have been applied for the analytic procedures. The hybrid technique of SMOTE-GA-MLP yields the highest performance overall.

Key contributions of this research in the area of skin lesion classification are now summarized. First, it specifies the exact type of a Spitz lesion, which is extremely difficult and challenging in real life. Second, it combines the results of previous works on the steps needed for the development of an automatic CAD system for Spitzoid lesion classification, in order to assist dermatopathologists during the diagnosis process. Third, our work makes a classification based on various testes and types of data such as: clinical, histological, and immunohistochemical data. Contrary to previous work in literature that only concentrate on microscopic vision which cannot give us an accurate classification. Finally, the analysis for differentiating

major classes of these lesions, namely SN (Spitz nevus) v. AST, is based on several features, including the immunohistochemical markers. Specifically, the findings indicate that localization of lesions, cytonuclear atypia, and Ki67 proliferative index are the most weighted features to differentiate AST from SN.

4.2 Implications of the Findings

As noted, we evaluated the scaled hospital dataset with seven (7) types of classifiers: K-NN, LR, DT, MLP, NB, RF and SVM. Where GA was applied, MLP achieves the highest accuracy at 0.98.

Three key observations and implications may be drawn from the results: (1) GA can correctly rank significant attributes since selected GA performs well in terms of classification performance; (2) SMOTE over-sampling method can perfectly solve the problem of our imbalanced data and overcome our model to biases towards majority classes; and (3) MLP outperformed all other linear and nonlinear classification methods with respect to accuracy performance indicators. Therefore, the model proposed for similar type SN v. AST analysis will be a model where SMOTE is used for solving class imbalance problem, GA is used for feature selection phase and MLP to be applied for the classification phase. The proposed SMOTE-GA-MLP structure has previously been provided in **Figure 2**.

In summary, the suggested system accomplished higher classification accuracy rate, by improving the data quality, solving class-imbalance problem, decreasing the number of attributes and obtaining higher performance rate, while identifying the most critical features that can influence the classification. Results obtained in this study prove that the SMOTE-GA-MLP CAD system is valuable in aiding the dermatologists to identify ASTs, and to make the correct diagnosis. Accordingly, extending beyond this work may demonstrate a huge capacity in the area of medical decisions making in skin lesion analysis.

4.3 Study Limitations & Future Works

This study has several limitations, most related to the data. First, the rarity of this disease and the lack of data in the hospitals about this type of lesions especially for the ASN case were an obstacle for us to collect enough data. We could use automatic data generation methods but we preferred to use only the real data to get realistic results. In our future work we aim to collect more real data and apply data generation methods to create new data from our real sampled data, and then we will compare results. Second, the nature of real-world skin lesion hospital datasets is not only imbalanced, but also heterogeneous and contains a lot of missing values and errors which can affect the analysis results. In our future work we will concentrate on improving the data quality by applying various existing techniques in literature for data preprocessing and find out the one more suitable to our data. Also we aim to add the third class of Spitzoid lesions which is: Spitz melanomas. It is a malignant melanoma that is histologically similar to a benign skin lesion which makes the classification more challenging.

Concerning the analytical side, our future work will involve comparing and integrating the very promising approaches for classification, such as the ensemble techniques, by integrating multiple simple classifiers based on bagging, boosting, and stacking methods to improve the classification accuracy of Spitzoid lesions.

5. REFERENCES

- Aličković, E., & Subasi, A. (2017). Breast cancer diagnosis using GA feature selection and Rotation Forest. *Neural Computing and Applications*, 28(4), 753-763.
- Al-Masni, M. A., Al-antari, M. A., Choi, M. T., Han, S. M., & Kim, T. S. (2018). Skin lesion segmentation in dermoscopy images via deep full resolution convolutional networks. *Computer methods and programs in biomedicine*, 162, 221-231.

- Bach, M., Werner, A., Żywiec, J., & Pluskiewicz, W. (2017). The study of under-and over-sampling methods' utility in analysis of highly imbalanced data on osteoporosis. *Information Sciences*, 384, 174-190.
- Bledsoe, W. W. (1961). The use of biological concepts in the analytical study of systems. In *ORSA-TIMS national meeting*.
- Blum, A., Rassner, G., & Garbe, C. (2003). Modified ABC-point list of dermoscopy: a simplified and highly accurate dermoscopic algorithm for the diagnosis of cutaneous melanocytic lesions. *Journal of the American Academy of Dermatology*, 48(5), 672-678.
- Breiman, L. (2001). Random forests. *Machine learning*, 45(1), 5-32.
- Chawla, N. V., Bowyer, K. W., Hall, L. O., & Kegelmeyer, W. P. (2002). SMOTE: synthetic minority over-sampling technique. *Journal of artificial intelligence research*, 16, 321-357.
- Cleophas, T. J., & Zwinderman, A. H. (2016). Clinical data analysis on a pocket calculator. *Springer*. Retrieved from doi, 10, 978-3.
- Ebrahimzadeh, E., Foroutan, A., Shams, M., Baradaran, R., Rajabion, L., Joulani, M., & Fayaz, F. (2019). An optimal strategy for prediction of sudden cardiac death through a pioneering feature-selection approach from HRV signal. *Computer methods and programs in biomedicine*, 169, 19-36.
- Firoze, A., & Rahman, R. M. (2015). Mining ICDDR, B hospital surveillance data and exhibiting strategies for balancing large unbalanced datasets. *International Journal of Healthcare Information Systems and Informatics (IJHISI)*, 10(1), 39-66.
- Gambhir, S., Malik, S. K., & Kumar, Y. (2018). The Diagnosis of Dengue Disease: An Evaluation of Three Machine Learning Approaches. *International Journal of Healthcare Information Systems and Informatics (IJHISI)*, 13(3), 1-19.
- Han, H., Wang, W. Y., & Mao, B. H. (2005, August). Borderline-SMOTE: a new over-sampling method in imbalanced data sets learning. In *International conference on intelligent computing* (pp. 878-887). Springer, Berlin, Heidelberg.
- Han, W., Huang, Z., Li, S., & Jia, Y. (2019). Distribution-Sensitive Unbalanced Data Oversampling Method for Medical Diagnosis. *Journal of medical systems*, 43(2), 39.
- Harms, K. L., Lowe, L., Fullen, D. R., & Harms, P. W. (2015). Atypical Spitz tumors: a diagnostic challenge. *Archives of pathology & laboratory medicine*, 139(10), 1263-1270.
- He, H., Bai, Y., Garcia, E. A., & Li, S. (2008, June). ADASYN: Adaptive synthetic sampling approach for imbalanced learning. In *2008 IEEE International Joint Conference on Neural Networks (IEEE World Congress on Computational Intelligence)* (pp. 1322-1328). IEEE.
- Holland, J. H. (1992). *Adaptation in natural and artificial systems: an introductory analysis with applications to biology, control, and artificial intelligence*. MIT press.
- Houari, R., Bounceur, A., Kechadi, T., Tari, A., & Euler, R. (2016, November). Missing Data Analysis Using Multiple Imputation in Relation to Parkinson's Disease. In *Proceedings of the International Conference on Big Data and Advanced Wireless Technologies* (p. 32). ACM.
- Jain, S., & Pise, N. (2015). Computer aided melanoma skin cancer detection using image processing. *Procedia Computer Science*, 48, 735-740.

- Majid, A., Ali, S., Iqbal, M., & Kausar, N. (2014). Prediction of human breast and colon cancers from imbalanced data using nearest neighbor and support vector machines. *Computer methods and programs in biomedicine*, 113(3), 792-808.
- Mathew, J., Pang, C. K., Luo, M., & Leong, W. H. (2018). Classification of imbalanced data by oversampling in kernel space of support vector machines. *IEEE transactions on neural networks and learning systems*, 29(9), 4065-4076.
- Moscarella, E., Lallas, A., Kyrgidis, A., Ferrara, G., Longo, C., Scalvenzi, M., ... & Tomasini, C. (2015). Clinical and dermoscopic features of atypical Spitz tumors: a multicenter, retrospective, case-control study. *Journal of the American Academy of Dermatology*, 73(5), 777-784.
- Nguyen, H. M., Cooper, E. W., & Kamei, K. (2009, November). Borderline over-sampling for imbalanced data classification. In *Proceedings: Fifth International Workshop on Computational Intelligence & Applications* (Vol. 2009, No. 1, pp. 24-29). IEEE SMC Hiroshima Chapter.
- Pedrosa, A. F., Lopes, J. M., Azevedo, F., & Mota, A. (2016). Spitz/Reed nevi: a review of clinical-dermatoscopic and histological correlation. *Dermatology practical & conceptual*, 6(2), 37.
- Puyalnithi, T., & Vankadara, M. (2018). A Unified Feature Selection Model for High Dimensional Clinical Data Using Mutated Binary Particle Swarm Optimization and Genetic Algorithm. *International Journal of Healthcare Information Systems and Informatics (IJHISI)*, 13(4), 1-14.
- Roffman, D., Hart, G., Girardi, M., Ko, C. J., & Deng, J. (2018). Predicting non-melanoma skin cancer via a multi-parameterized artificial neural network. *Scientific reports*, 8(1), 1701.
- Rubegni, P., Tognetti, L., Pellegrino, M., Burrioni, M., Fimiani, M., Miracco, C., ... & Cevenini, G. (2016, May). Spitz nevus versus atypical Spitz tumor: Objective morphological differentiation by digital dermoscopy analysis. In *2016 IEEE International Symposium on Medical Measurements and Applications (MeMeA)* (pp. 1-5). IEEE.
- Satheesha, T. Y., Satyanarayana, D., Prasad, M. G., & Dhruve, K. D. (2017). Melanoma is skin deep: a 3D reconstruction technique for computerized dermoscopic skin lesion classification. *IEEE journal of translational engineering in health and medicine*, 5, 1-17.
- Spitz, S. (1948). Melanomas of childhood. *The American journal of pathology*, 24(3), 591.
- Sulit, D. J., Guardiano, R. A., & Krivda, S. (2007). Classic and Atypical Spitz Nevi: Review of the literature-Response.
- Turgut, S., Dağtekin, M., & Ensari, T. (2018, April). Microarray breast cancer data classification using machine learning methods. In *2018 Electric Electronics, Computer Science, Biomedical Engineering's Meeting (EBBT)* (pp. 1-3). IEEE.
- Vapnik, V. (1998). *Statistical Learning Theory*. John Wiley&Sons. Inc., New York.
- World Health Organization. (2018). WHO Classification of Skin Tumours.
- Xie, F., Fan, H., Li, Y., Jiang, Z., Meng, R., & Bovik, A. (2017). Melanoma classification on dermoscopy images using a neural network ensemble model. *IEEE transactions on medical imaging*, 36(3), 849-858..
- Yu, M. T. S. (2015). Data Mining for Bioinformatics: Design with Oversampling and Performance Evaluation. *Journal of Medical and Biological Engineering*, 35(6), 775-782.

